European Review for Medical and Pharmacological Sciences 2018; 22: 4146-4155

CT quantitative analysis study for angiogenesis, and degree of ischemic necrosis and glucose metabolite in non-small cell lung cancer

M. JIANG[1], H.-Y. LU[2], X.-H. SHAN[1], W. XU[1], X.-D. GENG[1], C. LU[1], J.-H. CHEN[3]

[1]Department of Radiology, Affiliated People's Hospital of Jiangsu University, Zhenjiang City, Jiangsu Province, China
[2]School of Medicine, Jiangsu University, Jiangsu, China
[3]Department of Pathology, Affiliated People's Hospital of Jiangsu University, Zhenjiang City, Jiangsu Province, China

Min Jiang and Haoyue Lu contributed equally as first author

Abstract. – OBJECTIVE: We aimed at exploring the feasibility of noninvasive late arterial phase enhanced CT imaging in evaluating tumor angiogenesis, ischemic necrosis, and glucose metabolism, thereby providing pathological information for the comprehensive treatment plan in non-small cell lung cancer (NSCLC).

PATIENTS AND METHODS: 52 cases of NSCLC were enrolled in this study. The mean ischemia necrosis CT quantitative value (INCTQ) and CT enhanced value (CTe) of the tumor were determined, and the immunohistochemical staining of factors relating to tumor angiogenesis, ischemic necrosis and glucose metabolism, including VEGF, VEGFR-2, HIF-1α, CAIX, GLUT1, and GLUT3, were conducted.

RESULTS: The mean INCTQ values of different expression grades of VEGF, VEGFR-2, HIF-1α, and CAIX have no significant difference, but the mean INCTQ values of different expression grades of GLUT1 or GLUT3 have significant differences ($p < 0.001$), respectively. However, INCTQ value has a positive correlation with CAIX expression. In addition, CTe value was positively correlated with VEGF.

CONCLUSIONS: To sum up, late arterial phase CT enhanced images of NSCLC not only can assess the tumor angiogenesis, but also can reflect the degree of ischemic necrosis, effectively reflecting the level of glucose metabolism in tumor and tumor angiogenesis, for the comprehensive treatment program.

Key Words
Computed tomography angiography, NSCLC, Angiogenesis effect, Glucose, Necrosis.

Introduction

Lung cancer is a widespread global malignant neoplasm responsible for more than 1 million deaths annually worldwide[1]. The frequency of lung cancer is rising every year, in younger people especially. Thus, this has aroused attention to investigate lung cancer extensively[2]. Most of the patient's at the first visit were in advanced stage of lung cancer, so they missed out the best possible surgical treatment. For more effective treatment plans, a deep understanding of the molecular mechanisms of tumorigenesis is required. Tumor growth and development depend on the angiogenesis and the degree of necrosis within the tumor is associated with the extent of the hypoxia and angiogenesis[3,4]. Hypoxia phenomenon existed within the malignant microenvironment. Tumor internal hypoxia is the result of the faster tumor tissue growth because of increased number of cells and the lack of effective blood supply results in decreased oxygen concentration[5,6]. Tumor cells in order to adapt to the hypoxia microenvironment, through gene induction, expression and regulation and other signaling pathway to escape the apoptosis and promote the tumor growth and metastasis and tumor angiogenesis[5,6]. In recent years, as medical technology continues to advance, the medical research and treatment program has made some important breakthroughs. There are several invasive and non-invasive methods to identify the hypoxia in NSCLC. It has been reported that contrast-enhanced Computed Tomography (CT) allows the assessment of the tumor angiogenesis[7] and it is also used to identify the necrosis within the tumor[8]. This non-invasive technique can precisely and rapidly identify the tumor vascularity and also has the potential to assess the tumor aggressiveness in patients with NSCLC. Thus, we investigate the probable correlation between the necrosis tissues or tumor angiogenesis displayed in enhanced CT images, with marker expression of the hypoxia and angiogenesis in NSCLC. We aim to find potential targets for therapy in non-small cell lung cancer (NSCLC).

Corresponding Author: Xiuhong Shan, MD; e-mail: xiuhongshan112@163.com

Patients and Methods

Patients

Preoperative CT scan of 52 patients with non-small cell lung cancer was collected at Zhenjiang First People's Hospital, Affiliated to Jiangsu University (Affiliated Renmin Hospital of Jiangsu University) from December 2010 to May 2013. All the patients had not received radiation or chemical treatment before CT examination. The patient's age ranged from 39 to 87 years (the mean age was 61.6 years), 36 males and 16 females. Among them, 18 cases were diagnosed as squamous cell carcinoma, 31 cases as adenocarcinoma, and 3 cases as adenosquamous cell carcinoma. CT examinations were performed at intervals of 1-8 days before the surgical operation. The paraffin-embedded tissue specimens of NSCLC were preserved in the Department of Pathology. The study was approved by the Research Ethics Committee of the hospital. All patients enrolled in the study gave informed consent for all investigations.

CT Imaging Scheme

We used 64-slice (SOMATOM Sensation, Siemens, Germany) and 256-slice CT (Brilliance iCT, Philips, Amsterdam, The Netherlands) scanner system. The contrast agent was iodixanol with iodine concentration of 300 mg/mL. The CT scans were carried out before and 35 s after administration with iodixanol at the rate of 3 mL/s and 2 mL/kg through the antecubital vein. Scan thicknesses were 0.5 mm (256-slice CT) or 0.625 mm (64-slice CT), pitch=1, the reconstruction images thicknesses were 3 mm at axial, coronal, and sagittal orientations.

Image Data Acquisition Method

Measurement of ischemia necrosis CT quantifies value (INCTQ): the maximum slices of lesions at axial, coronal, and sagittal were displayed with 50/250 (window centre/window width). At the three images of enhanced sequence, we measured the CT value (HN) and size area (SN) of lower density regions in tumor, and also measured the CT value (HC) and size area (SC) of moderate density regions in tumor. The lower density regions were regarded as the ischemic necrosis regions of tumor, and the moderate density regions were regarded as the non-ischemic areas (Figure 1). The value of INCTQ was calculated using the formula as follows: (HC/HN)×(SN/SC). CT enhancement value (CTe) measurement: the CT values of the non-necrotic area in the largest section of the lesions were measured, and the CTe can be achieved by subtracting the CT value of plain images from the CT value of enhanced images (Figure 2). All the data were measured by 3 radiologists independently.

Evaluation of MVD

MVD measurement: we calculated microvessel density of the tumor stained with CD34, which is an endogenous marker[9]. All the brown staining cells or cluster endothelial cells which differed from neighboring microvasculature, tumor cells or others tissues, were regarded as single and countable microvessels. The lumen size was larger than 8 red blood cell diameter and thicker muscular layers were not counted. We documented the mean value by counting 5 continuous fields of microvessels.

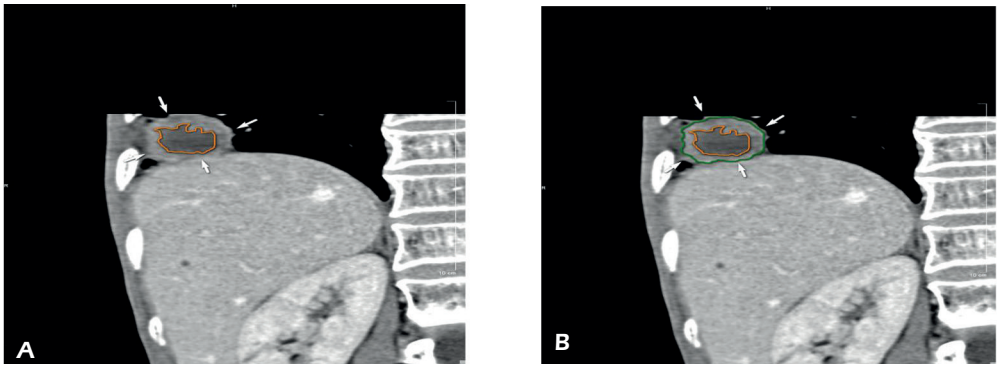

Figure 1. Measurement of INCTQ on the contrast-enhanced CT image of lung cancer. CT images with 3 mm slice thickness and the tumor in the centermost region (where white mark arrows pointing towards the tumor): we examined the contour of the tumor at 50/250, distinctive between the enhanced area and non-enhanced area. **A**, We illustrate the outline of the non-enhanced area by the red line and recorded the CT value as (HN) and necrosis size as (SN). **B**, The enhanced section is the area between the green and red line; the CT value was recorded as (HC) and non-necrosis size as (SC).

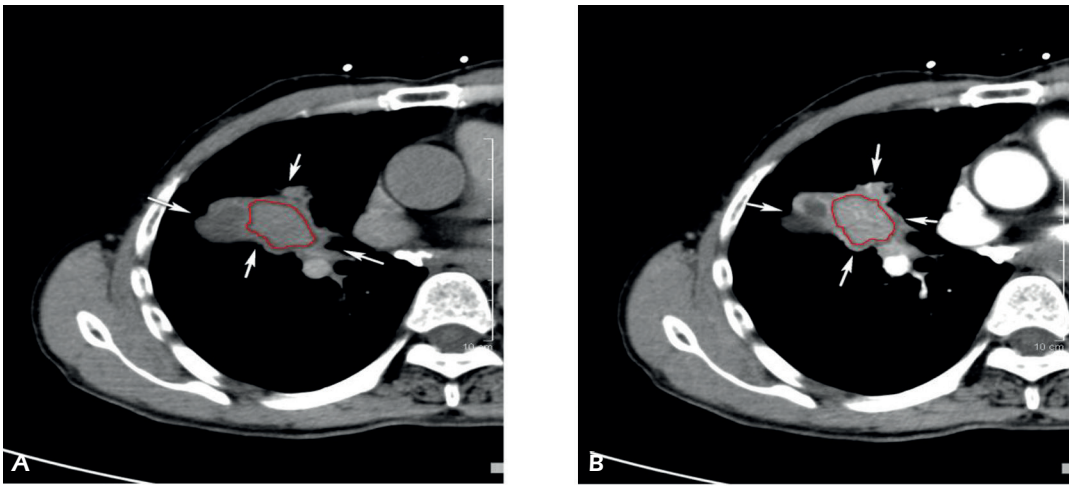

Figure 2. Lung lesion (white arrow point to the tumor) measured CT value of unenhanced area. **A**, The same level of the enhanced CT image. **B**, Avoiding low-density necrosis and edge, we drew a red circle as interest area, CTe = enhanced CT value (**B**) - unenhanced CT value (**A**).

Immunohistochemical Staining and Evaluation

Immunohistochemical staining was performed with routine two-step immunohistochemical technique. The immunoreactivity of genes was scored according to the method by Ozbudak et al[10]. The expression of genes of tumor cells, including GLUT1, GLUT3, CAIX, VEGF, VEFGR 2, and HIF-1α, was graded from 0 to 2. The absence of brown staining of tumor cells was referred as negative expression, grade 0; brown staining of tumor cells: ≤ 20% positive cells were referred as grade 1; > 20% positive cells were referred as grade 2. We observed the slide under a magnification of 10×40, and documented the mean value by counting 5 continuous fields of microvessels.

Statistical Analysis

Statistical analysis was carried out by using software SPSS 17.0 (SPSS Inc., Chicago, IL, USA). The differences of the MVD, CTe and INCTQ values of different GLUT1, GLUT3, HIF-1α, CAIX, VEGF and VEGE-R2 expression grades were tested by one-way analysis of variance (ANOVA); if the variance was heterogeneity by test, the mathematical correction was performed. The pairwise comparison was conducted by Bonferroni post hoc test. The correlations of microvessel density (MVD), CTe, and INCTQ value were tested by using Spearman rank correlation. $p<0.05$ was regarded as statistically significant.

Results

CT Image Data of NSCLC, Pathological Diagnosis

52 cases of NSCLC, aged between 39 to 87 years, mean 61.56±10.67 years, 36 males and 16 females, were investigated. Among them, 31 patients were diagnosed as adenocarcinoma, 17 patients as squamous cell carcinoma, 4 patients as adenosquamous carcinoma pathologically diagnosed with expression grades of GLUT1, GLUT3, CA IX, HIF-1α, VEGF, and VEGFR-2. The mean values of MVD, CTe, and tumor INCTQ were shown in Table I.

NSCLC Angiogenesis

Microvascular density (MVD) evaluated by CD34 analysis

52 cases of NSCLC showed different microvascular distribution, CD34 was not significantly expressed in tumor stroma except for microvascular endothelial cells. The irregular tubular shape and beaded-like endothelial cells, small clusters endothelial cells and scattered endothelial cells were located at tumor area (Figure 3). MVD values ranged from 4 to 66, with an average of 27.54 ± 15.74 (Table I).

Expression of VEGF and VEGFR-2 in NSCLC

VEGF and VEGFR-2 expressed in the cytoplasm of tumor cells in NSCLC were shown as brown staining in Figure 4A and 4B. The VEGF

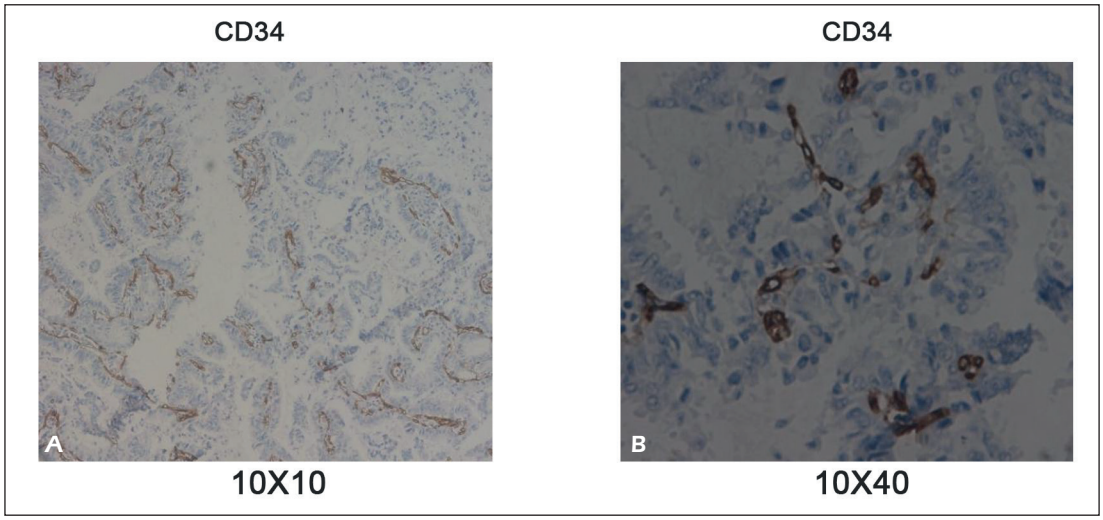

Figure 3. Immunohistochemical staining of CD34 in NSCLC tissue revealed microvascular distribution. There were various shapes of brown staining endothelial cells between tumor cells.

expression was evaluated based on the percentage of positive cells. The positive expression rate of VEGF and VEGFR-2 was 71.2% (37/52) and 73.1% (38/52), respectively (Table I).

Association of INCTQ with VEGF, VEGF-R2, and MVD expression in NSCLC

One-way ANOVA analysis showed that there were no significant differences in the INCTQ mean values for different VEGF (p = 0.440) and VEGFR-2 expression grades (p = 0.319) (Table II), respectively. Bonferroni tests showed that there were also no significant between subgroups of VEGF and VEGFR-2 expression (Table III). Spearman's rank correlation analysis showed that there was no correlation between INCTQ and MVD (r = -0.062, p=0.661) (data not shown).

Table I. Pathological information of patients.

Category	Mean/Count		Category	Mean/Count	
Gender	Female	16	VEGF	0	15
	Male	36		1	16
Age		61.56±10.67		2	21
INCTQ		0.95±1.03	VEGFR 2	0	14
CTe		26.47±11.64		1	12
MVD		27.54±15.74		2	26
HIF-1α	0	14	Pathology	WDAC	3
	1	20		MDAC	11
	2	18		PDAC	17
GLUT1	0	15		WDSCC	3
	1	13		MDSCC	9
	2	24		PDSCC	5
GLUT3	0	16		PDASC	4
	1	20			
	2	16			
CAIX	0	27			
	1	12			
	2	13			

WDSCC: Well differentiated squamous cell carcinoma; MDSCC: Moderately differentiated squamous cell carcinoma; PDSCC: Poorly differentiated squamous cell carcinoma; WDAC: Well differentiated adenocarcinoma; MDAC: Moderately differentiated adenocarcinoma; PDAC: Poorly differentiated adenocarcinoma; PDASC: Poorly differentiated adenosquamous cell carcinoma.

Table II. Comparison of INCTQ and CTe between subgroups of Gender, GLUT1, GLUT3, CAIX, VEGF, VEGFR 2 and pathology.

		INCTQ		CTe	
		Mean±SD	*p*	Mean±SD	*p*
Gender	Female	0.97±1.27	0.916	29.33±11.03	0.619
	Male	0.9±40.93		25.19±11.83	
HIF-1α	0	0.58±0.66	0.249	32.26±12.64	0.091
	1	1.18±1.29		24.43±11.80	
	2	0.97±0.90		24.22±9.53	
GLUT1	0	0.35±0.23	<0.001	29.25±11.65	0.516
	1	0.52±0.55		26.35±12.33	
	2	1.55±1.20		24.79±11.43	
GLUT3	0	0.39±0.28	<0.001	27.41±10.09	0.288
	1	0.69±0.61		28.73±13.16	
	2	1.84±1.34		22.71±10.80	
CAIX	0	0.69±0.77	0.149	28.48±12.38	0.180
	1	1.10±1.27		27.51±11.86	
	2	1.34±1.19		21.32±8.73	
VEGF	0	1.08±1.32	0.440	20.73±9.39	0.064
	1	0.67±0.69		29.71±12.79	
	2	1.07±1.02		28.09±11.19	
VEGFR 2	0	1.21±1.29	0.319	27.81±11.86	0.727
	1	1.11±1.33		24.21±12.52	
	2	0.73±0.65		26.78±11.44	
Pathology	WDAC	0.37±0.14	0.027	26.20±10.34	0.146
	MDAC	1.34±1.24		23.70±12.55	
	PDAC	0.40±0.35		26.29±11.46	
	WDSCC	1.95±0.97		25.67±19.05	
	MDSCC	0.86±0.63		26.30±9.29	
	PDSCC	1.76±1.71		32.36±13.52	
	PDASC	1.07±1.38		28.65±14.03	

WDSCC: Well differentiated squamous cell carcinoma; MDSCC: Moderately differentiated squamous cell carcinoma; PDSCC: Poorly differentiated squamous cell carcinoma; WDAC: Well differentiated adenocarcinoma; MDAC: Moderately differentiated adenocarcinoma; PDAC: Poorly differentiated adenocarcinoma; PDASC: Poorly differentiated adenosquamous cell carcinoma.

Association of CTe with VEGF/VEGF-R2 and MVD expression in NSCLC

One-way ANOVA analysis showed that there were no significant differences in the CTe mean values for different VEGF ($p = 0.064$) and VEGFR-2 expression grades ($p = 0.727$) (Table II), respectively. However, Bonferroni test showed that the levels of CTe in grade 0 were higher than that in grade 1 ($p=0.093$) and 2 ($p=0.176$), respectively (Table III). Spearman's rank correlation analysis showed that there was no correlation between CTe and MVD, though higher CTe value was associated with higher MVD value ($r = 0.148$, $p=0.294$) (data not shown).

Expression of HIF-1α, CAIX, GLUT1, and GLUT3

The expression of HIF-1α was characterized by brown staining in the nuclei of the tumor cell (Figure 4C). The percentage of positive expression was 73.1% (38/52), in which the numbers of expression grades 0, 1, and 2 were 14, 20, and 18, respectively (Table I). The CAIX expression showed focal membranous brown staining (Figure 4D). The CAIX positive tumor cells were

Table III. Pairwise comparison of INCTQ and CTe values between two different grades of VEGF or VEGFR-2 using Bonferroni post-hoc test.

	INCTQ	CTe
VEGF		
0 vs. 1	0.825	0.093
0 vs. 2	> 0.999	0.176
1 vs. 2	0.748	> 0.999
VEGFR-2		
0 vs. 1	> 0.999	> 0.999
0 vs. 2	0.494	> 0.999
1 vs. 2	0.882	> 0.999

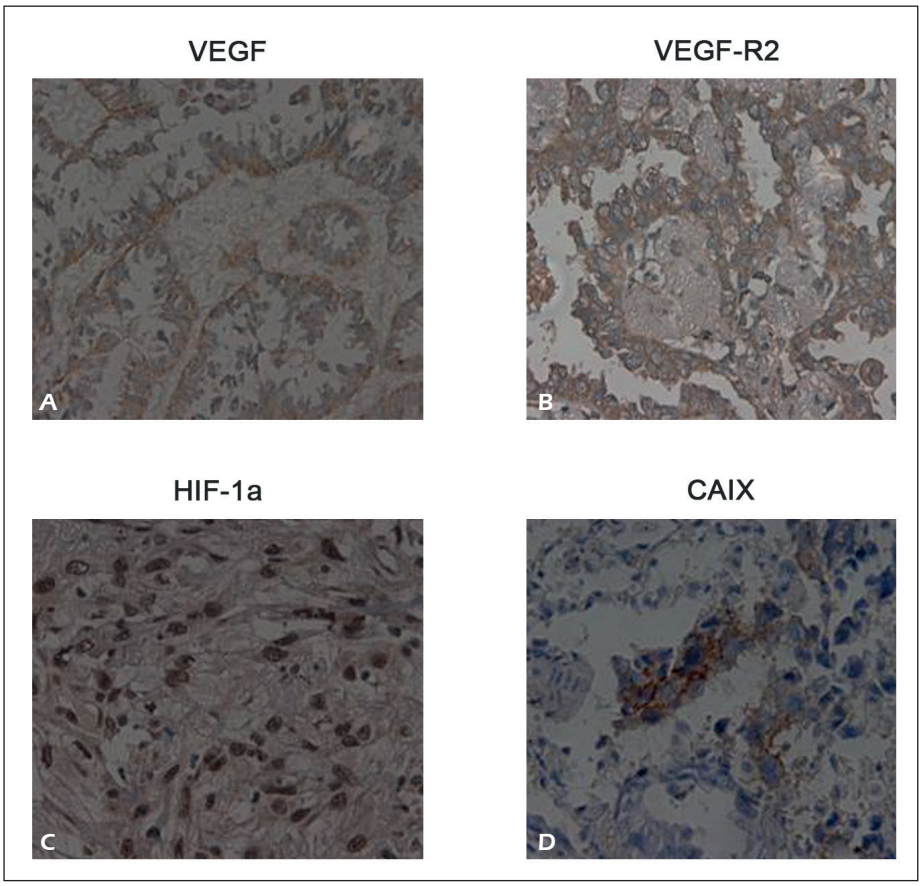

Figure 4. Immunochemical staining for VEGF, VEGF-R2, HIF-1α, and CAIX in NSCLC tissue. Positive starting of VEGF (**A**) and VEGF-R2 (**B**) was showed in the cytoplasm of tumor cells. **C**, HIF-1α expression existed in the nuclei of tumor cells. (**D**) CA IX expression was showed focal membranous brown staining and the positive tumor cells were distributed mainly around the necrotic area.

mainly distributed around the necrotic area and accounted for 48.1% (25/52). The numbers of expression grades 0, 1, and 2, were 27, 12, and 13, respectively (Table I). GLUT1 expression displayed membranous brown staining of local tumor cells, positive tumor cells were mainly

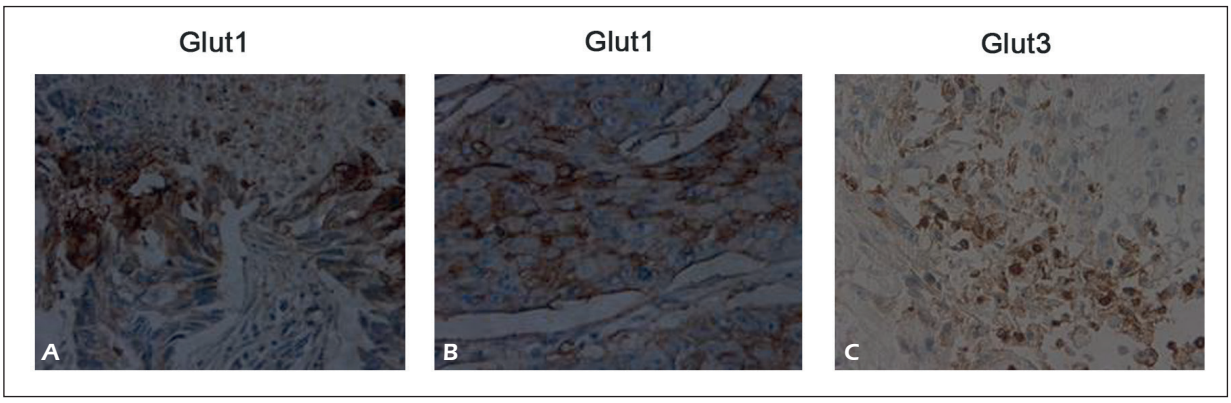

Figure 5. Immunochemical staining for GLUT1 and GLUT3 in NSCLC. **A**, Positive GLUT-1 expression was observed in tumor cells around necrotic areas. **B**, Positive tumor cells with expression of GLUT1 dispersed in capillary scarce regions. **C**, Positive tumor cells expression of GLUT3 was inflammatory cells and some stromal cells with membranous and cytoplasmic brown staining in necrotic areas.

distributed around necrotic areas and at scarce capillary regions (Figure 5A and 5B). The percentage of GLUT1 positive expression was 71.2% (37/52), and the numbers of expression grade 0, 1, and 2 were 15, 13, and 24, respectively (Table I). GLUT3 positive tumor cells expressions were inflammatory cells and stromal cells distributed in the necrotic areas, but very few tumor cells were brown stained (Figure 5C). The positive expression of GLUT3 was 69.2% (36/52) and the numbers of the expression grades 0, 1, and 2 were 16, 20, and 16, respectively (Table I).

Association of INCTQ values with HIF-1α, CAIX, GLUT1, and GLUT3

INCTQ mean values for different HIF-1α, GLUT1, GLUT3, and CAIX expression grades were showed in Table II. One-way ANOVA analysis showed that there were no significant differences in the INCTQ mean values for different HIF-1α expression grades (p= 0.249) (Table II). There were significant differences in the INCTQ mean values for different GLUT1 and GLUT3 expression grades (p = <0.001), respectively. Bonferroni test showed that the INCTQ value of GLUT1 expression grade 2 was significantly higher than that of grade 0 (p<0.001) and 1 (p=0.004) (Table IV). The INCTQ value of GLUT3 expression grade 2 was significantly higher than that of grade 0 (p<0.001) and 1 (p<0.001) (Table IV). One-way ANOVA analysis showed that there were no significant differences in the INCTQ mean values for different CAIX expression grades (p = 0.149) (Table II). Notably, INCTQ mean value of HIF-1α and CAIX co-expression, single expression and no expression were 1.40 ± 1.31 (n = 19), 0.75 ± 0.15 (n = 25) and 0.51 ± 0.74 (n = 8). One-way ANOVA analysis showed that there were significant differences (F = 3.260, p= 0.047) (data not shown).

Table IV. Pairwise comparison of INCTQ and CTe values between two different grades of VEGF or VEGFR-2 using Bonferroni post-hoc test.

	INCTQ	CTe
HIF-1α		
0 vs. 1	0.294	0.158
0 vs. 2	0.867	0.155
1 vs. 2	> 0.999	> 0.999
Glut 1		
0 vs. 1	> 0.999	> 0.999
0 vs. 2	< 0.001	0.759
1 vs. 2	0.004	> 0.999
GLUT3		
0 vs. 1	0.889	> 0.999
0 vs. 2	< 0.001	0.769
1 vs. 2	< 0.001	0.383
CAIX		
0 vs. 1	0.745	> 0.999
0 vs. 2	0.189	0.211
1 vs. 2	> 0.999	0.552

Association of CTe values with HIF-1α, GLUT1, GLUT3, and CAIX

CTe mean values for different HIF-1α, GLUT1, GLUT3, and CAIX expression grades were showed in Table II. One-way ANOVA analysis showed that there were no significant differences in the CTe mean values for different HIF-1α expression grades (p= 0.091) (Table II). There were no significant differences in the CTe mean values for different GLUT1 (p = 0.516), GLUT3 (p = 0.288), and CAIX (p = 0.180) expression grades (Table II), respectively. However, Bonferroni test showed that the CTe value of HIF-1α expression grade 0 was higher than that of grade 2 (p=0.155) (Table IV). However, Bonferroni test also showed no differences in CTe values between all two grades for GLUT1, GLUT3 and CAIX expression (Table IV). Further analysis showed that CTe mean values of HIF-1α and CAIX coexpression, single expression and no expression were 23.32 ± 10.45 (n = 19), 25.84 ± 10.92 (n = 25) and 35.93 ± 12.92 (n = 8), respectively. One-way ANOVA analysis showed that there were significant differences (F = 3.736, p= 0.031) (data not shown).

Association of pathology with INCTQ and CTe values

Among the subgroups of pathology, there were significant differences in INCTQ values (p=0.027) but not in CTe values (p=0.146) (Table II). The INCTQ values in patients with WDAC and PDAC were significantly lower than that in other groups and there were no significant differences between any two subgroups (data not shown).

Discussion

Numerous researches[11-13] showed that hypoxia microenvironment plays a very important role in the growth and development of malignant solid tumors including lung cancer. In tumor cells influenced by hypoxia factors such as HIF-1α,

the process of mitochondrial oxidative phosphorylation was suffered from different degrees of inhibition compared with oxygen metabolism of mitochondria, and glycolysis metabolism was relatively inefficient with one molecule of glucose generating only 2 ATP [6,14]. Even if the mitochondrial oxidative phosphorylation is inhibited, in order to escape apoptosis, many chronic hypoxic tumor cells eventually increase glucose transport through the synthesis of GLUT1 or GLUT3 and supplement sufficient energy through glycolysis metabolic pathway[15-17]. Although the cancer cells down-regulate the expression of GLUT1 through the inhibition of oxidative phosphorylation, the HIF-1 induced GLUT1 overexpression is still very strong[18]. The abnormal expression of GLUT1 was confirmed in tumor tissue from many reports. In March 2010, Airley et al[19] detected a variety of tumor tissues with tissue microarray. The expression of GLUT1 was mainly expressed around the necrotic area which further showed that the expression of GLUT1 was closely related to the hypoxia and necrosis[20]. Under the hypoxic condition, there are different degrees of tumor angiogenesis and glycolysis metabolism in different tumors. This may be associated with tumor angiogenesis and GLUT1 expression degree, some showed significant necrosis, and some shown homogeneity[21,22]. Literature[23-25] reported that the expression of CAIX in the malignant solid tumors such as renal cell carcinoma, gastric carcinoma, lung cancer, and cervical carcinoma were significantly enhanced. The most important function of CAIX is through the hydration of carbon dioxide to maintain intracellular alkaline environment and extracellular acidic environment[23,24]. The expression of CAIX was regulated by HIF-1α, and the expression was mainly concentrated in the tumor necrosis area. Moreover, the expression level was positively correlated with the degree of hypoxia[26]. At the same time, tumor angiogenesis also provides essential nutrients for tumor growth. VEGF is an effective angiogenic factor, which is up-regulated in many tumors playing a major contribution to the tumor angiogenesis[27,28]. VEGF, also known as vital growth factor for vascular endothelial, during the hypoxic condition HIF-1α, acts as the primary controller of VEGF[29,30]. VEGF not only plays an important role in the growth and metastasis of tumor, but also has a certain effect on the proliferation and apoptosis of tumor cells[31]. The density resolution of CT image is higher and can be used to evaluate the loose necrotic area of tissue sensitively; late arterial phase-enhanced imaging showed a greater contrast between the necrotic and non-necrotic area[32]. In the late arterial phase enhanced stage, the contrast agent doesn't get through the extravascular space and remains inside the blood vessels, so it can better determine the degree of microvascular distribution. In this study, we retrospectively analyzed the relationships between parameters of CT and the degree of tumor necrosis and angiogenesis, GLUT1 and GLUT3 expression in NSCLC cases confirmed by pathology. According to the method for measuring the degree of necrosis in the lesion by Antoch et al[33], we determined factors of necrosis area to evaluate ischemic necrosis degree, and measured INCTQ on the late arterial phase enhanced CT images and found that, when INCTQ value was larger, the degree of necrosis was higher. The results of this research indicated that INCTQ had a strong correlation with GLUT1 and GLUT3 ($p<0.001$). When GLUT1 and/or GLUT3 expression was higher, the level of glucose metabolism was higher; therefore, INCTQ can better reflect the level of glucose metabolism in tumor tissue. The INCTQ value has no significant correlation with the expression of HIF-1α and was higher in patients with positive expression of CAIX. Furthermore, the results showed that CTe value was positive correlated with VEGF expression. These results may be related to the upregulation of both tumor angiogenesis and glucose metabolism for resistance of tumor necrosis. On the other hand, they may promote the initiation of apoptotic pathways. Thus, according to late arterial phase, CT enhanced images for measuring INCTQ can reflect the degree of tumor tissue necrosis and glucose metabolism in tumor tissue.

Conclusions

The high correlation between ischemia necrosis CT quantitative values (INCTQ) of NSCLC and GLUT1 or GLUT3 suggests that INCTQ value can reflect the degree of lung cancer tissue ischemia necrosis accurately since GLUT1 and GLUT3 expressions are the indicators of the tumor glycolysis metabolism. In addition, the late arterial phase CT enhanced value (CTe) of NSCLC has a positive correlation with VEGF expression, suggesting the capability of CTe value in evaluating tumor angiogenesis.

Acknowledgements
This work was supported by Natural Science Foundation of Jiangsu (Grant No. BK20151334); Zhenjiang Innovation Capacity Project (Grant No. SS2015023)

Conflict of Interest
The Authors declare that they have no conflict of interests.

References

1) Parkin DM, Bray F, Ferlay J, Pisani P. Global cancer statistics, 2002. CA Cancer J Clin 2005; 55: 74-108.
2) Jemal A, Tiwari RC, Murray T, Ghafoor A, Samuels A, Ward E, Feuer EJ, Thun MJ; American Cancer Society. Cancer statistics, 2004. CA Cancer J Clin 2004; 54: 8-29.
3) Duffy JP, Eibl G, Reber HA, Hines OJ. Influence of hypoxia and neoangiogenesis on the growth of pancreatic cancer. Mol Cancer 2003; 2: 12.
4) Chen WT, Huang CJ, Wu MT, Yang SF, Su YC, Chai CY. Hypoxia-inducible factor-1α is associated with risk of aggressive behavior and tumor angiogenesis in gastrointestinal stromal tumor. Jpn J Clin Oncol 2005; 35: 207-213.
5) Kondoh M, Ohga N, Akiyama K, Hida Y, Maishi N, Towfik AM, Inoue N, Shindoh M, Hida K. Hypoxia-induced reactive oxygen species cause chromosomal abnormalities in endothelial cells in the tumor microenvironment. PLoS One 2013; 11: e80349.
6) Bel Aiba RS, Dimova EY, Görlach A, Kietzmann T. The role of hypoxia inducible factor-1 in cell metabolism--a possible target in cancer therapy. Expert Opin Ther Targets 2006; 10: 583-599.
7) Cuenod CA, Fournier L, Balvay D, Guinebretière JM. Tumor angiogenesis: pathophysiology and implications for contrast-enhanced MRI and CT assessment. Abdom Imaging 2006; 31: 188-193.
8) sHypoxia-selective targeting by the bioreductive prodrug AQ4N in patients with solid tumors: results of a phase I study. Clin Cancer Res 2008; 14: 1096-1104.
9) Semaan A, Munkarah AR, Arabi H, Bandyopadhyay S, Seward S, Kumar S, Qazi A, Hussein Y, Morris RT, Ali-Fehmi R. Expression of GLUT-1 in epithelial ovarian carcinoma: correlation with tumor cell proliferation, angiogenesis, survival and ability to predict optimal cytoreduction. Gynecol Oncol 2011; 121: 181-186.
10) Ozbudak IH, Karaveli S, Simsek T, Erdogan G, Pestereli E. Neoangiogenesis and expression of hypoxia-inducible factor 1alpha, vascular endothelial growth factor, and glucose transporter-1 in endometrioid type endometrium adenocarcinomas. Gynecol Oncol 2008; 108: 603-608.
11) Wang J, Tian L, Khan MN, Zhang L, Chen Q, Zhao Y, Yan Q, Fu L, Liu J. Ginsenoside Rg3 sensitizes hypoxic lung cancer cells to cisplatin via blocking of NF-κB mediated epithelial-mesenchymal transition and stemness. Cancer Lett 2018; 415: 73-85.
12) Graves EE, Maity A, Le QT. The tumor microenvironment in non-small-cell lung cancer. Semin Radiat Oncol 2010; 20: 156-163.
13) Riffle S, Pandey RN, Albert M, Hegde RS. Linking hypoxia, DNA damage and proliferation in multicellular tumor spheroids. BMC Cancer 2017; 17: 338.
14) Domenis R, Bisetto E, Rossi D, Comelli M, Mavelli I. Glucose-modulated mitochondria adaptation in tumor cells: a focus on ATP synthase and inhibitor factor 1. Int J Mol Sci 2012; 13: 1933-1950.
15) Airley RE, Mobasheri A. Hypoxic regulation of glucose transport, anaerobic metabolism and angiogenesis in cancer: novel pathways and targets for anticancer therapeutics. Chemotherapy 2007; 53: 233.
16) Wilson DF, Harrison DK, Vinogradov SA. Oxygen, pH, and mitochondrial oxidative phosphorylation. J Appl Physiol 2012; 113: 1838-1845.
17) Yu S, Zhao T, Guo M, Fang H, Ma J, Ding, Wang F, Chan P, Fan M. Hypoxic preconditioning up-regulates glucose transport activity and glucose transporter (GLUT1 and GLUT3) gene expression after acute anoxic exposure in the cultured rat hippocampal neurons and astrocytes. Brain Res 2008; 1211: 22-29.
18) Hayashi M, Sakata M, Takeda T, Yamamoto T, Okamoto Y, Sawada K, Kimura A, Minekawa R, Tahara M, Tasaka K, Murata Y. Induction of glucose transporter 1 expression through hypoxia-inducible factor 1alpha under hypoxic conditions in trophoblast-derived cells. J Endocrinol 2004; 183: 145-154.
19) Airley R, Evans A, Mobasheri A, Hewitt SM. Glucose transporter Glut-1 is detectable in peri-necrotic regions in many human tumor types but not normal tissues: study using tissue microarrays. Ann Anat 2010; 192: 133-138.
20) Valeria M, Franco G, Malgorzata R, Stefanie O, Martin P, Carla RB. Hypoxia-related marker GLUT-1, CAIX, proliferative index and microvessel density in canine oral malignant neoplasia. PLos One 2016; 11: e0149993.
21) Yoshimura H, Dhar DK, Kohno H, Kubota H, Fujii T, Ueda S, Kinugasa S, Tachibana M, Nagasue N. Prognostic impact of hypoxia-inducible factors 1α and 2α in colorectal cancer patients correlation with tumor angiogenesis and cyclooxygenase-2 expression. Clin Cancer Res 2004; 10: 8554-8560.
22) Bos R, van Diest PJ, de Jong JS, Van dGP, Van dVP, Van dWE. Hypoxia-inducible factor-1alpha is associated with angiogenesis, and expression of bFGF, PDGF-BB, and EGFR in invasive breast cancer. Histopathology 2005; 46: 31-36.
23) Loncaster JA, Harris AL, Davidson SE, Logue JP, Hunter RD, Wycoff CC Pastorek J, Ratcliffe PJ, Stratford IJ, West CM. Carbonic anhydrase (CA IX) expression, a potential new intrinsic marker of hypoxia: correlations with tumor oxygen measurements and prognosis in locally advanced carcinoma of the cervix. Cancer Res 2001; 61: 6394-6399.
24) Giatromanolaki A, Koukourakis MI, Sivridis E, Pastorek J, Wykoff CC, Gatter K, Harris AL. Expression of hypoxia-inducible carbonic anhydrase-9 relates to angiogenic pathways and independently

to poor outcome in non-small cell lung cancer. Cancer Res 2001; 61: 7992-7998.
25) Olive PL, Aquino-Parsons C, MacPhail SH, Liao SY, Raleigh JA, Lerman MI, Stanbridge EJ. Carbonic anhydrase 9 as an endogenous marker for hypoxic cells in cervical cancer. Cancer Rese 2001; 61: 8924-8929.
26) Pinheiro C, Sousa B, Albergaria A, Paredes J, Dufloth R, Vieira D, Schmitt F, Baltazar F. GLUT1 and CAIX expression profiles in breast cancer correlate with adverse prognostic factors and MCT1 overexpression. Histol Histopathol 2011;26 10: 1279-1286.
27) Oh SH, Kim WY, Lee OH, Kang JH, Woo JK, Kim JH, Glisson B, Lee HY. IGFBP-3 suppresses VEGF expression and tumor angiogenesis in head and neck squamous cell carcinoma. Cancer Sci 2012; 103: 1259-1266.
28) Koh YJ, Kim HZ, Hwang SI, Lee JE, Oh N, Jung K, Kim M, Kim KE, Kim H, Lim NK, Jeon CJ, Lee GM, Jeon BH, Nam DH, Sung HK, Nagy A, Yoo OJ, Koh GY. Double antiangiogenic protein, DAAP, targeting VEGF-A and angiopoietins in tumor angiogenesis, metastasis, and vascular leakage. Cancer Cell 2010; 18: 171-184.
29) Shemirani B, Crowe DL. Hypoxic induction of HIF-1α and VEGF expression in head and neck squamous cell carcinoma lines is mediated by stress activated protein kinases. Oral Oncol 2002; 38: 251-257.
30) Nishida T, Kondo S, Maeda A, Kubota S, Lyons KM, Takigawa M. CCN family 2/connective tissue growth factor (CCN2/CTGF) regulates the expression of Vegf through Hif-1α expression in a chondrocytic cell line, HCS-2/8, under hypoxic condition. Bone 2009; 44: 24-31.
31) Déry MAC, Michaud MD, Richard DE. Hypoxia-inducible factor 1: regulation by hypoxic and non-hypoxic activators. Int J Biochem Cell Biol 2005; 37: 535-540.
32) Shan X, Wang D, Chen J, Xiao X, Jiang Y, Wang Y, Fan Y. Necrosis degree displayed in computed tomography images correlated with hypoxia and angiogenesis in breast cancer. J Comput Assist Tomogr 2013; 37: 22-28.
33) Antoch G, Vogt FM, Veit P, Freudenberg LS, Blechschmid N, Dirsch O, Bockisch A, Forsting M, Debatin JF, Kuehl H. Assessment of liver tissue after radiofrequency ablation: findings with different imaging procedures. J Nucl Med 2005; 46: 520-525.